ELSEVIER

Polymer 43 (2002) 3109–3114

polymer

www.elsevier.com/locate/polymer

Physical and functional characterization of PHA_{SCL} membranes

Norma Galego[a,c], Flavio C. Miguens[b], Rubén Sánchez[a,*]

[a]*Advanced Material Laboratory, Polymer Section, North Fluminense State University, Av. Alberto Lamego 2000 Campos, R.J., CEP 28015-620, Campos dos Goytacates, Brazil*

[b]*Center of Biology and Biotechnology, North Fluminense State University, Campos dos Goytacates, Brazil*

[c]*Faculty of Chemistry, Havana University, Zapata and G, Havana 10400, Cuba*

Abstract

Dense semicrystalline membranes of polyhydroxyalkanoates with medium change length (PHA_{SCL}), polyhydroxybutyrate (PHB) and poly β (hydroxybutyrate-*co*-hydroxyvalerate) [P(βHB-*co*-XβHV)] were characterized using wide-angle X-ray (WAXS) and scanning electron microscopy. PHB membranes showed a more rugged surface than those of copolymers (0–22%HV). Properties such as swelling capacity, vapor permeability and selectivity were investigated. Swelling percentage in water–ethanol mixtures was 34% for PHB as compared to 14% for copolymers membranes. The ethanol/water selectivity (α_s) of PHB was 5.8 which shows that it is more selective than copolymers.

The water vapor and ethanol vapor permeability were determined by a gravimetric technique at different temperatures by static and dynamic methods. PHB permeability was 69.5 Barrer at 30 °C and a discreet increment was observed at temperatures (30–50 °C). The difference in permeability between PHB and [P(βHB-*co*-*X*%βHV)] could be interpreted in terms of the crystallization rate, crystallite size and distribution which impact to transport properties of amorphous phase.

Keywords: Polyhydroxyalkanoates; Membranes; Water vapor permeability

1. Introduction

With the advance of science and technology of polymeric membranes there has been an increasing demand for better quality separation processes. Here, membranes may be considered the ideal medium for separation processes [1]. While the principles used in membrane process have been known for over 150 years, it was only in the last 40 years that a burst occurred in synthetic membrane development driven by strong technological needs and commercial expectations. Since then the membrane separation science has experienced a tremendous progress which successfully broadened its application range [2].

The dominant application of membranes is certainly the separation of mixed phases or fluids, either homogeneous or heterogeneous. Separation of a mixture can be achieved if the difference in the transport coefficients of the components of interest is sufficiently large. Membranes can also be used in catalytic reactors, energy storage and conversion systems, as well as in key components of artificial organs, support for electrodes, or even to control the rate release of both useful and dangerous species. Membrane materials should combine functional properties like high permeability and selectivity as well as structural properties such as chemical and thermal stability besides good mechanical properties. All these properties should also be fitted to specific operating conditions. The possibility of meeting this set of characteristics is directly associated with the nature of the material used for the membrane [2]. In this regard, polymeric materials offer several advantages. Actually, polymeric membranes are dominant in commercial separation processes and have important role in a variety of industries such as chemical, biotechnological, pharmaceutical and food processing [1].

The water vapor permeability of polymers is an important characteristic when they are used as protective coatings for insulating and packing materials. Data on the swelling, diffusion and permeability of polymers are needed both for selection of the materials and also for predicting the service life in moist media.

Polymers of bacterial origin, like the polyhydroxyalkanoates (PHAs), are characterized as biocompatible 'green' thermoplastic [3] being biodegraded in specific treatment systems. The distinct feature of this PHAs family is that its biodegradation rate in moist air is negligible and therefore the PHAs should last long enough for most end uses as membrane in special process where this property is relevant. Another feature is the PHAs semicrystallinity, which helps to increase their chemical resistance. As far as permeability is concerned,

* Corresponding author. Tel.: +55-24-726-3725; fax: +55-24-726-3733.
E-mail address: sanchez@zappa.uenf.br (R. Sánchez).

0032-3861/02/$ - see front matter
PII: S0032-3861(02)00107-6

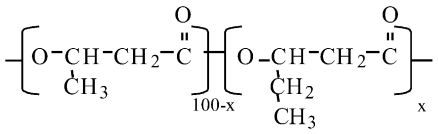

Fig. 1. Chemical structure of PHA_{SCL} where (x) is the HV contents.

few data have been published about the transport properties of short chain length polyhydroxyalkanoates (Fig. 1).

Mas et al. [4] prepared dense membranes for pervaporation from polyhydroxybutyrate (PHB) and copolymers hydroxybutyrate–hydroxyvalerate [P(βHB-*co*-*X*%βHV)] ($9 \leq X \geq 22\%$). They studied the swelling processes of P(βHB-*co*-9%βHV) in water–ethanol mixtures and reported swelling percentages, in pure water (0.6%) and pure ethanol (10.3%). The method used was not suitable to observe differences with other polymers.

Iordanskii et al. [5] studied sorption–diffusion indexes of the PHB–water system in a temperature range of 303–333 K. The temperature dependence of water vapor sorption and diffusion in PHB was investigated. Equilibrium sorption and diffusion kinetics were determined by a quartz Mac Bain's vacuum microbalance technique. The authors [5] determined the enthalpy of free water sorption as 12 kJ/mol and attributed this relatively low heat effect of sorption to be a characteristic of polymers possessing moderate hydrophobicity.

The main aim of the present work is to make a morphological characterization and to study the transport properties of dense membranes of PHB and P(βHB-*co*-*X*%βHV), where $0 \leq X \geq 22\%$.

2. Experimental

Materials. All PHA_{SCL} used were obtained from Aldrich Chemical Company, Inc. They were first purified by dissolution in chloroform and then precipitated in ethyl ether.

The molecular weights were determined by gel permeation chromatography (GPC). PHB; $M_n = 87{,}000$, P(βHB-*co*-8%βHV); $M_n = 92{,}000$, P(βHB-*co*-14%βHV); $M_n = 56{,}000$ and P(βHB-*co*-22%βHV); $M_n = 100{,}000$ Da.

GPC studies were carried out using a Lachrom Merck-Hitachi system with refractive index detector and PS 4000, PS400, PS40 and PS4 Licrogel columns placed in series with exclusion limits 10^6, 10^5, 10^4 and 10^3 Da. Chloroform was used as eluent at a flow rate of 1.0 ml/min and injection volumes of 20 μl were used. Polystyrene standards (Merck) with low polydispersity were used for the calibration curve.

Membrane preparation. Membranes of 2×2 cm were prepared by casting chloroform solution (1% w/v) at 45 °C, in a close Pyrex plate. After slow solvent evaporation each membrane received a thermal treatment at 80–90 °C during 4–6 h and was then stored in dry atmosphere to complete crystallization. The membrane thickness was found to be about 0.04–0.07 mm depending on the solution concentration. They were used after 10 days of preparation when the material did not show changes in diffractogram spectrum (DXR) [6].

Swelling measurement. The sorption capacity of the membranes was measured by immersing in ethanol–water solution of different concentration at 30 °C for 4 days. The swelling degree, S, was then calculated by:

$$S = [(m - m_0)/m_0] \times 100 \quad (1)$$

where m is the mass of the swollen sample and m_0 is the original mass.

Gravimetric Measurement of the permeability (P). The experimental determination of permeability was carried out in a small bottle, filled to half with the liquid and hermetically closed with the membrane (similar to the Payne cup). This bottle was enclosed in a reservoir, which had silica gel or molecular sieves, so that the relative vapor into the reservoir was set to zero. This reservoir was placed into a bath at constant temperature. The small bottle was weighted, from time to time to attain equilibrium (24 h).

The permeability (P) is the amount of permeant passing through a polymer film of unit thickness, per unit area, per unit time and at a drop pressure. It was determined from Eq. (2) [7] as Barrer unit; 10^{-10} [cm^3 (STP) cm cm^{-2} s cm Hg^{-1}].

$$P = \frac{(\text{quantity of permeant}) \times (\text{film thickness})}{(\text{area}) \times (\text{time}) \times (\text{pressure drop across the film})}. \quad (2)$$

Vapor permeability was also measured by dynamic permeation experiments as a function of time, using the time-lag method. In the last case, the following equation was used [9,10].

$$(LQ_t/P_vA) \cong DH[t - L^2/6D] \quad (3)$$

where L is the membrane thickness; Q_t is the permeated mass in the time (hours) t; P_v is the vapor pressure difference across the membrane; D is the diffusivity; H is the Henry's law coefficient and the product $DH = P$ is the permeability of the membrane.

The slope of the plot LQ_t/P_vA vs. t at steady state gives the permeability by unit area (A) and the time-lag was calculated from the intercept for $(LQ_t/P_v) = 0$. Where $D = L^2/6\Theta$ and Θ is the time-lag.

Membrane crystallinity. Membrane crystallinity studies were performed by wide-angle X-ray (WAXS), on PHA_{SCL} membrane samples. A Seifert-FPM model URD65 X-ray generator with a Ni filter to provide a Cu Kα radiation ($\lambda = 0.1542$ nm) was used. Every scan was recorded in the range of $2\theta = 6$–$36°$ at a scan speed of 0.01°/10 s. Crystallinity percentages were calculated from samples of equal weight. Crystalline peaks were well-defined in the X-ray diffractogram, as can be seen in the Fig. 2, and the degree of crystallinity X_c were obtained from the plot in the normalized diffractogram shown by the relationship

$$X_c = [(\text{total area}) - (\text{amorphous area})]/(\text{total area})$$

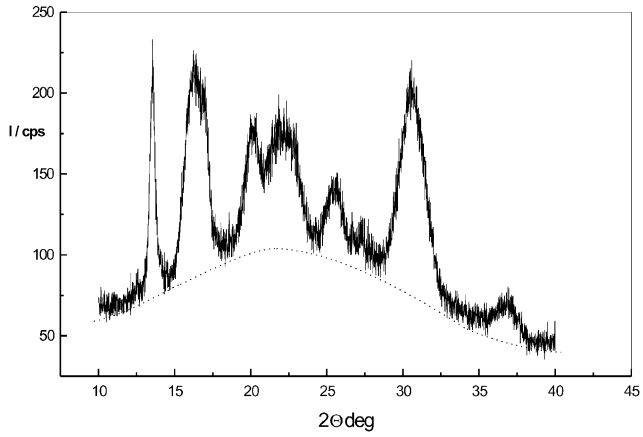

Fig. 2. X-ray diffractogram of PHB membrane where the dash line area correspond to amorphous area.

All the samples were aged to obtain a top crystallization. It was monitored until reach crystallization equilibrium up to 10 days [11,12].

Scanning electron microscopy. The surface and cross-section region of PHA membranes were studied by scanning electron microscopy using a Zeiss 692, SEM. The cross-section region was exposed by fracture in liquid nitrogen. Samples were prepared with conductor Ag or double face graphite adhesive and sputter coated with approximately 20 nm of Pd–Au. The membranes were sensitive when subfetted to the electron beam at 15–25 keV to obtain a high resolution, it break out frequently if not exposed a short time.

3. Results and discussion

The crystallinity of the PHA_{SCL} membranes obtained from diffractogram like the one in Fig. 2 are presented in Table 1. It can be noted that the PHA_{SCL} dense membranes are highly crystalline. Moreover the DXR analysis for copolymers ($0 \leq X \geq 22\%$) showed a slight tendency of the crystallinity to decrease with the percentage of HV increment in the copolymers.

The upper surface of the membranes, i.e. the membrane face of evaporation to air, could be analyzed and compared from SEM micrographs (Fig. 3). The PHA_{SCL} surfaces show some kind of rugged structure which is more pronounced for PHB membranes that present more defects or voids as observed in Figs. 3(a) and 4(a), for the same cast conditions.

Table 1
PHA_{SCL} membranes crystallinity

Polymer	Crystallinity percentage
PHB	62.1 ± 0.3
P(βHB-*co*-8%βHV)	60.9 ± 0.3
P(βHB-*co*-14%βHV)	59.6 ± 0.8
P(βHB-*co*-22%βHV)	57.8 ± 0.3

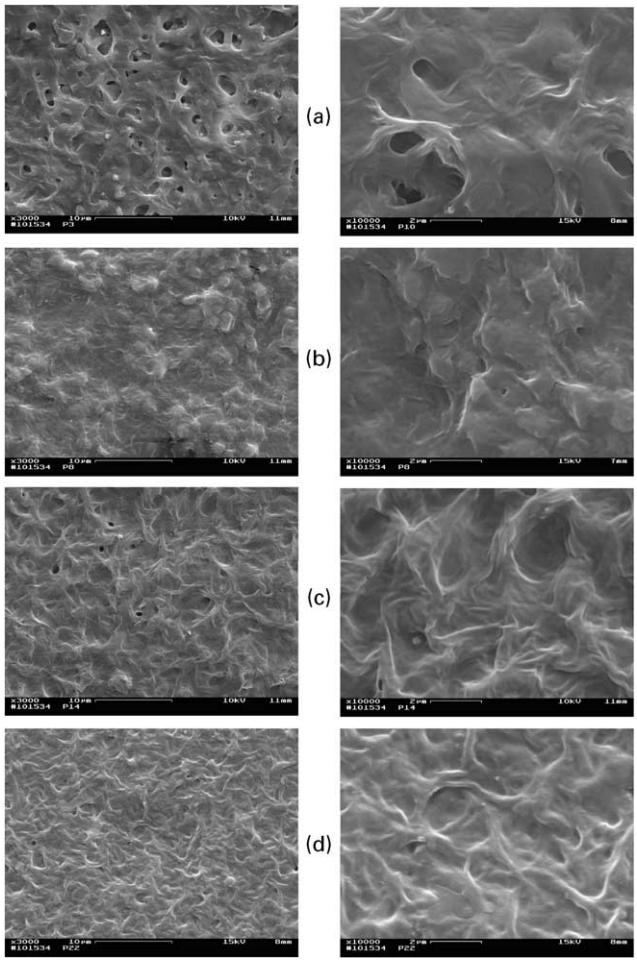

Fig. 3. Scanning electron micrographs of PHB (a), P(βHB-*co*-8%βHV) (b), P(βHB-*co*-14%βHV) (c) and P(βHB-*co*-22%βHV) (d) membranes.

These features were also observed by Mas et al. [4] for dense membranes of PHB, P[βHB-*co*-9%βHV] and P[βHB-*co*-22%βHV].

Other relevant detail was the cross-section of PHB and P[βHB-*co*-22%βHV], Fig. 4(a) and (b), which is more regular for the copolymer and tends to form a more compact membrane.

The differences observed in the morphology between homo and copolymers could be discuss from the crystallinity properties. The PHA_{SCL}, between 0 and 22%HV contents, had the same crystallinity percentage and crystallize in a similar manner without any significative change in the lattice parameters by HV contribution.

Abey et al. [13] reported for PHA_{SCL} that the nucleation and crystal growth rate reflect the size increment and the perfection of spherulites. From the Mitomo et al. [14] density study of crystalline and amorphous phases for P[βHB-*co*-*X*%βHV] ($0 \leq X \geq 100$), it can be concluded that the crystalline phase densities remain almost constant from 0 to 22%HV. On the other hand the amorphous phase densities decrease linearly as the HV composition increased. It was also reported that the crystallization rate

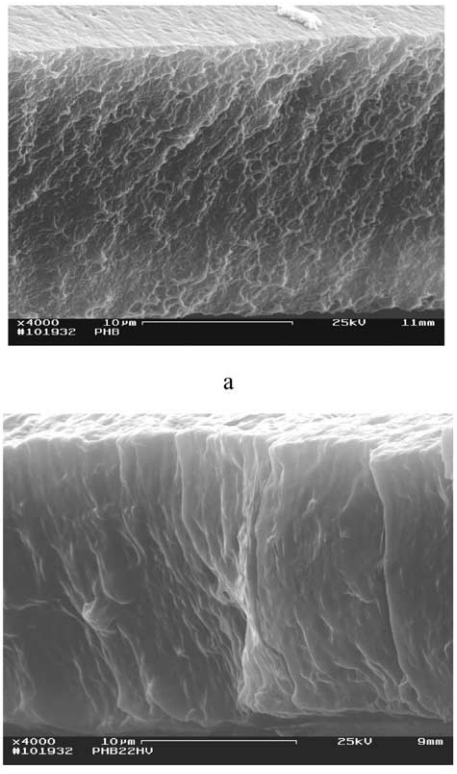

Fig. 4. Cross-section scanning electron micrographs of PHB (a) and P(βHB-*co*-22%βHV) (b) membranes.

of copolymers are slower than homopolymer PHB cast films from solution [11–13]. Copolyesters do not crystallize in the elapsed time in which evaporation of solvent occurs, and consequently they form a complete amorphous film at this initial step. After chloroform evaporation, uniform spherulites with different crystallite size and distribution may be formed through the copolymer with the subsequent impact into the amorphous phase.

The swelling percentages of PHA_{SCL} membranes, shown in Fig. 5, from different ethanol–water mixture, present a significative difference to ethanol between PHB and P[βHB-*co*-*X*%βHV]. The higher ethanol swelling percentages of the homopolymer, could also be explained from the crystallization rate that introduces microstructural phase differences in the polymers. These differences are revealed more sharply from the value of the sorption selectivity (α_s) parameter.

Sorption selectivity of the PHB membranes calculated from swelling degree (*S*) using Eq. (4), gave a value of $\alpha_s = 5.8$ ethanol moles per water mole absorbed (Fig. 6).

$$\alpha_s = [S(\text{pure water})/MW_{H_2O}]/[S(\text{pure ethanol})/MW_{C_2H_5OH}] \quad (4)$$

where $MW_{H_2}O$ is the water molecular weight (18 Da) and $MW_{C_2}H_5OH$, ethanol molecular weight (46 Da).

As expected, this reflects the ethanol greater specific swelling behavior of PHB in relation to that of the copolymers.

Water and ethanol vapor permeability of the different PHA_{SCL} membranes were studied by a gravimetric method. This method was employed with two different procedures and both procedures insure the reliability of the measurement in semicrystalline polymers.

The time-lag procedure has been successfully applied to rubbery polymers but in some cases it gave unreliable results for semicrystalline polymers due to boundary layer effects [9]. In any case, the T_g (glass transition temperature) of PHA_{SCL} is below room temperature. Therefore, the PHA_{SCL} amorphous phase is in a rubbery state, which can contribute to the good agreement between the static and dynamic measurements.

Static and dynamic measurements of the water vapor permeability, Table 2 and Fig. 7, are in a good agreement. In particular the PHB water vapor permeability (Fig. 7) obtained from time-lag measurements at different temperatures (30–50 °C) presents a small change in slope, indicating its weak dependence with temperature. Furthermore, the permeability of PHB was higher than that of P[βHB-*co*-22%βHV] at 30 °C.

The time-lag studies could also provide a diffusion coefficient (*D*), if one supposes a weak dependence of the permeant concentration across the membrane. Due to the scarce data in *D* vs. concentration [5] for PHAs, Eq. (3)

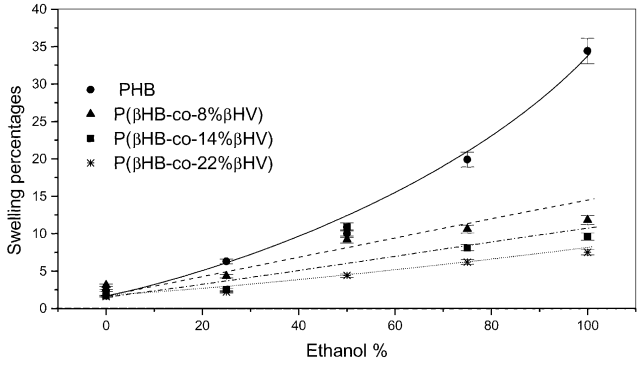

Fig. 5. The swelling percentage for PHA_{SCL} membranes in water–ethanol mixtures.

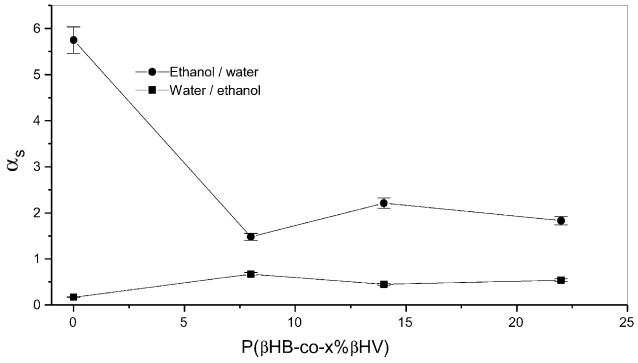

Fig. 6. Water/ethanol sorption selectivity (α_s) for PHA_{SCL} membranes.

Table 2
Water vapor permeability by static (P_{static}) and dynamic ($P_{dynamic}$) measurements for PHB and P(βHB-*co*-22%βHV) membranes (thickness 0.0045 cm) and dynamic measurements of diffusivity (D) and time-lag (Θ) at different temperatures

Polymer	T (°C)	P_{static} (Barrer)	$P_{dynamic}$ (Barrer)	$D \times 10^9$ (cm^2 s^{-1})	Θ (h)
PHB	30	67.7	69.5	1.11	0.85
PHB	40	77.8	80.6	1.36	0.69
PHB	50	77.8	79.3	1.38	0.68
P(βHB-*co*-22%βHV)	30	59	61.6	1.32	0.71

was used as an approximated way to calculate diffusion coefficients.

The values of the diffusion coefficients for PHB in Table 2 show very little trend with temperature. On the other hand, these D values are comparable to copolymer (22%HV) in spite of the fact that the copolymer permeability is lower. This fact could be related to solubility factors, which are ruling the permeability ($P = DH$) PHA_{SCL} behavior.

In another set of static measurements was found that the water permeability difference between PHB and its copolymers (Fig. 8) when increasing temperature, is more pronounced for copolymers with higher HV contents (14 and 22%) and almost constant for PHB and P(βHB-8%βHV). This behavior could be a consequence of microstructural differences that induce a change of the diffusion coefficient with temperature, as the HV content is increased.

All these experimental evidences allow one to consider the permeability behavior as a consequence of the modification of the amorphous region due to the different size and distribution of crystallites in the membranes. These crystallites could then be assumed to function as fillers and affect diffusion coefficient as a consequence of the more tortuous nature of the diffusion path [15].

The selectivity of the membrane (α_p) (Table 3) defined by the ratio of the two vapor permeabilities [2] ($\alpha_{1,2} = P_1/P_2$) was calculated from water and ethanol vapor permeability for the PHA_{SCL}. In the case of PHB, this membrane presented an ambiguous permeability and swelling behavior, which is not characteristic of copolymers. In fact, PHB molecular layer in contact with liquid ethanol swells due to the more expressive solid–liquid adsorption considering that the ethanol sorbate solubility parameter ($\delta_{ethanol} = 12.9$) is higher than the corresponding for water ($\delta_{water} = 23.5$) [17]. This justifies a higher affinity of PHB to liquid ethanol.

In the case of copolymers, the difference could be discussed as a consequence of the surface characteristic discussed above. In contrast, the water in vapor phase presented more accessibility to the polymer structure due to its lower molecular size. The small water molecule acts as a structure probe, which is sensitive to the morphology of the PHB. An additional consideration is the more specific hydrogen-bonding interaction between the water and the PHB structure. The water molecules are tightly immobilized by H-bonds with ester group [16], which increases the permeation across the membrane.

The permeability decreases when the interactive forces between polymer and moisture smaller than the cohesive forces between the water molecules. In this case the water will tend to aggregate and form clusters as it was reported in polypropylene membranes [15].

The PHB transport behavior can be compared in terms of barrier properties with other semicrystalline hydrophobic polymers, such as PET [7] and PP [7]. Table 4 presents a

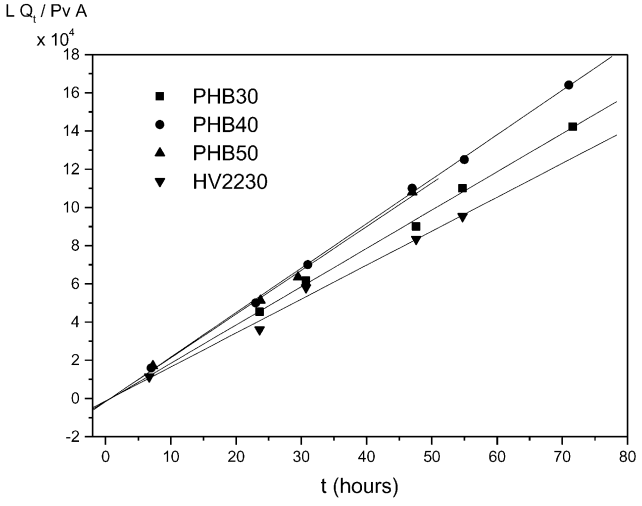

Fig. 7. Time-lag plot from water vapor measurements of PHB membranes at 30, 40, and 50 °C and P(βHB-*co*-22%βHV) membranes at 30 °C.

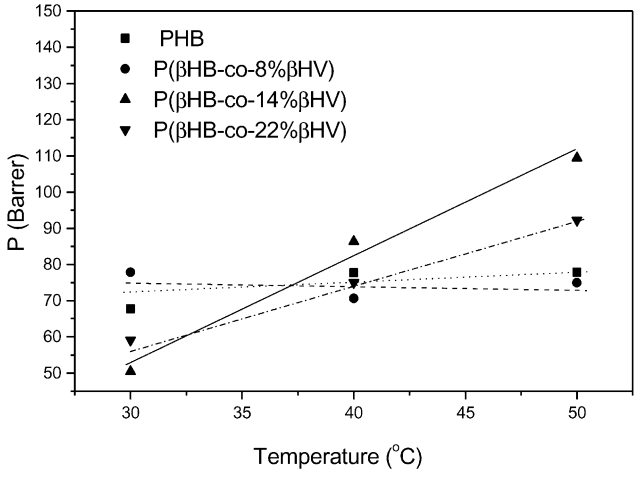

Fig. 8. The PHA_{SCL} membrane water vapor permeability (P) at different temperatures.

Table 3
PHB and P(βHB-*co*-22%βHV) membranes selectivity at 30 °C

Polymer	$P_{\text{water vapor}}$ (Barrer)	$P_{\text{ethanol vapor}}$ (Barrer)	α_p (P_{wv}/P_{ev})
PHB	67.7	10	6.8
P(βHB-*co*-22%βHV)	59	36.6	1.6

Table 4
Water vapor permeability coefficient (P) of semicristalline polymers

Polymer	Crystallinity (%)	T (°C)	Water vapor permeability (Barrer)
PHB	62	30	67.7
PP [7]	60–70	25	51
PET [7,17]	40	25	130

similar permeability of these polymers used for pervaporation on a laboratory scale for separation of water/acetone mixtures [17]. These results are mainly due to a high level of crystallinity and the related similar tortuosity and geometric impedance imposed by the crystallites to the diffusing species.

4. Conclusions

The PHA_{SCL} morphological characterization showed a rugged surface for these polymers which is more pronounced in PHB membranes. The morphology and permeability properties of PHA_{SCL} dense membranes are greatly influenced by their high crystallinity and different crystallization rate associated with polymer structure from cast process. The swelling and permeability behaviors are a consequence of the modification of the amorphous region due to the size and distribution of the crystallites in the membranes, which introduce more tortuous diffusion path.

The PHB presented a higher selectivity for water vapor permeation with respect to the ethanol and acetone, however, the copolymer membranes of P(βHB-*co*-*X*%βHV) did not show the same selectivity to water or ethanol vapor.

Acknowledgements

The authors would like to thank CNP and FAPERJ for their financial support.

References

[1] Burganos VN. MRS Bull 1999;24(3):19–20.
[2] Naylor TdeV. Rapra Rev Rep, Rep 89 1996;8(5):3–4.
[3] Lupke T, Radusch H-J, Metzner K. Macromol Symp 1998;127:227–40.
[4] Mas A, Jaaba H, Sledz J, Schue F. Eur Polym J 1996;32(4):435–40.
[5] Iordanskii AL, Kamaev PP, Zaikov GE. Int J Polym Mater 1998;41:55–63.
[6] Doi Y. Microbial polyesters. New York: VCH, 1990. 153p.
[7] Miguel O, Fernandez-Benedi MJ, Irvin JJ. J Appl Polym Sci 1997;64:1849–59.
[9] Neogi P. Diffusion in polymers. New York: Marcel Dekker, 1996. p. 173–7.
[10] Naylor TdeV. Comprehensive polymer science, Polymer Properties, vol. 2. New York: Pergamon Press, 1989. p. 645.
[11] Bluhm TL, Hamer GK, Marchessault RH, Fyfe CA, Veregin RP. Macromolecules 1986;19:2871–6.
[12] Bloembergn S, Holden DA, Hamer GK, Bluhm TL, Marchessault RH. Macromolecules 1986;19:2865–71.
[13] Abe H, Doi Y, Aoki H, Akehata T, Huri Y, Yamaguchi A. Macromolecules 1995;28:7630–7.
[14] Mitomo H, Morishita N, Doi Y. Polymer 1995;36(13):2573–8.
[15] Comyn J. Polymer permeability. New York: Elsevier Applied Science Publishers, 1986. p. 315.
[16] Razumovskii LP, Ioordanskii AL, Zikov GE, Zagreba ED, Mc Neill IC. Polym Degrad Stab 1994;44:171–5.
[17] Koros WJ, Fleming GK, Jordan SM, Kim TH, Hoerhn HH. Prog Polym Sci 1988;13:339–401.